Large in-stream wood yield during an extreme flood (Storm Alex, October 2020, Roya Valley, France): Estimating the supply, transport, and deposition using GIS

Guillaume Piton, Marianne Cohen, Myriam Flipo, Maciej Nowak, Margot Chapuis, Gabriel Melun, Yannick Robert, Nathalie Andréis, Frédéric Liebault

Large In-Stream Wood Yield during an extreme flood (Storm Alex, October 2020, Roya Valley, France): Estimating the Supply, Transport, and Deposition Using GIS

Guillaume Piton[*a], Marianne Cohen[b], Myriam Flipo[b], Maciej Nowak[b,c], Margot Chapuis[d], Gabriel Melun[e], Yannick Robert[f], Nathalie Andréis[g], Frédéric Liebault[a]

[a] Université Grenoble Alpes, INRAE, CNRS, IRD, Grenoble INP, IGE, 38000 Grenoble, France.
[b] Sorbonne Université, U.R. Médiations, 28 rue Serpente, 75006 Paris, France.
[c] Université Adam Mickiewicz de Poznań, Faculté de Biologie, ul. Uniwersytetu Poznańskiego 6, 61614 Poznań, Poland
[d] Université Côte d'Azur, CNRS, ESPACE, bd Edouard Herriot, 06204 Nice, France.
[e] Office Français de la Biodiversité, Direction de la Recherche et de l'Appui Scientifique, 12 cours Louis Lumière, 94300 Vincennes, France
[f] Service de Restauration des Terrains de Montagne de l'Isère, Office National des Forêts, 9 quai Créqui; 38026 Grenoble, France
[g] Service de Restauration des Terrains de Montagne des Alpes-Maritimes, Office National des Forêts, 62 av Giscard d'Estaing, 06205 Nice, France
* corresponding author: guillaume.piton@inrae.fr (Guillaume Piton)

This is the last draft version of the paper: Piton G, Cohen M, Flipo M, Nowak M, Chapuis M, Melun G, Robert Y, Andréis N, Liebault F. 2024. Large in-stream wood yield during an extreme flood (Storm Alex, October 2020, Roya Valley, France): Estimating the supply, transport, and deposition using GIS. Geomorphology **446** : 108981. DOI: 10.1016/j.geomorph.2023.108981

1 Introduction

The understanding of the large wood transport dynamics has proven to be highly important for flood risk management and the design of structures and infrastructure adapted to the specificities of mountain rivers (Lassettre and Kondolf, 2011; Ruiz-Villanueva et al., 2014, 2017; Gschnitzer et al., 2017; Mazzorana et al., 2018), as was also the case for the design of biodiversity preservation policies for the river corridors (Gurnell et al., 2002; Dufour et al., 2003; Wohl et al., 2019). In mountain streams, during morphogenic flooding, stream banks covered by riparian forests may be affected by erosion and channel migration processes (Church and Ferguson, 2015; Church and Jakob, 2020). Vegetation has colonized every available room, i.e. former farmland, pastureland, the streambanks and the active channel margins, when anthropogenic pressure diminishes, the intensity of flooding remains low, and/or sediment supply decreases (Piégay et al., 1994; Liébault et al., 2005; Astrade et al., 2011; Wohl et al., 2019). The active channels of alpine streams thus change in a pseudo-cyclic manner, progressively narrowing as a result of gradual colonization of alluvial deposits, then suddenly widening as a consequence of flood disturbance (Arnaud-Fassetta et al., 2005; Lallias-Tacon et al., 2017). This classic pattern of recovery to flood disturbances is superimposed on a more general trend of vegetation encroachment in active channels that started at the end of the Little Ice Age, and that accelerated after the Second World War under the primary effect of rural depopulation, catchment-scale reforestations and subsequent sediment supply decrease, often exacerbated by anthropogenic impacts of, e.g., reservoir dams and gravel mining (Liébault and Piégay, 2002; Liébault et al., 2005; Comiti, 2012).

In this context, the riparian trees, when recruited and transported by flooding, can become a risk factor, generating considerable damage along river corridors where human infrastructure is installed (Lucía et al., 2015; Mazzorana et al., 2011, 2018; Comiti et al., 2016; Okamoto et al., 2019), while its ecological and moderator functions are recognized and its preservation recommended (Piégay et al., 1994). Large quantities of in-stream wood resulting from the undermining and subsequent uprooting of riparian forests can contribute to the catastrophic nature of flooding by forming log jams obstructing certain structures and portions of channels, locally raising the level of flows and rerouting these flows toward the floodplain (Mazzorana et al., 2018; Okamoto et al., 2019; Ruiz-Villanueva et al., 2014, 2017). In certain very particular configurations that allow the accumulation of a large volume of water behind a large wood jam, rupture of the wood jam can generate a wood jam outburst, i.e., a dangerous flood wave

because it is sudden and loaded with large wood (see one of the rare documented examples by Macchione and Lombardo 2021).

Since riparian corridors of montane rivers are generally forested, their erosion implies that the river will recruit the plant biomass present on these areas, thus leading to the formation of large in-stream wood accumulations, defined in the present article as wood pieces >0.1 m in diameter and >1 m long (Braudrick et al. 1997). Bank erosion is the main mechanism of large wood recruitment in mountain streams, most particularly recent alluvial terraces that have long been colonized by riparian trees (Mazzorana et al., 2011; Comiti et al., 2016). Large wood can also come from landslides and torrential tributaries subjected to erosion and supplies from their stream banks, and more marginally from avalanche deposits or anthropogenic stocks such as deposits from sawmills and logging operations (Gasser et al., 2019; Friedrich et al., 2021).

Although knowledge of recruitment processes for large wood in rivers are improving e.g. thanks to monitoring campaigns (Ravazzolo et al., 2015; Piégay et al., 2017), the wood transport regime (transport frequency, wood sizes, mobility, transport distances) remains for the most part poorly understood (Ruiz-Villanueva et al., 2016; Wohl et al., 2019). A few major floods have been studied, providing estimations of the volumes of large wood produced (Rickenmann, 1997; SABO Division, 2000; Comiti et al., 2016; Lucía et al., 2018; Steeb et al., 2023). In the rarest cases, notably in Switzerland and Germany, estimations of the stocks supplied and deposited along a given river stretch made it possible to carry out crude assessments (Schmocker and Weitbrecht, 2013; Lucía et al., 2015; Steeb et al., 2017). Such analyses contribute to improving the comprehension of large wood dynamics in waterbodies.

The present article explores this line of investigation. It aims to measure the volume of the large wood fluxes, i.e., supply, deposit and transport, which occurred during the Storm Alex at the scale of the Roya River catchment (area: 394 km²). It details the approach retained to complete a large wood connectivity assessment and quantify the associated uncertainties. Since this type of assessment has not, to our knowledge, been conducted at this scale, the article provides the opportunity to show how certain GIS (Geographical Information System) and forestry data, that are typically available on a national scale, can be used to conduct this type of assessment. The complete application of the method to the case study of the Roya River subjected to the Storm Alex also makes it possible to better understand how large wood flux is organized through an intermediate-sized mountain watershed (<1,000 km²) subjected to extreme flooding. The article is organized into three main sections. Section 2 details the catchment area studied as well as the data and approaches used to carry out the assessment and qualify the uncertainties. Section 3 presents the results of the analysis. Section 4 discusses the uncertainties of the approach and broaden the perspective to other catchments and the use of empirical formula to predict such large wood supply.

2 Material and methods

2.1 2.1 The Storm Alex and the Roya River catchment

The Alpes-Maritimes department in France underwent an extreme precipitation event from mid-day on October, 2nd 2020 to early morning on October 3rd: an exceptionally large warm advection from the Mediterranean caused exceptional precipitation on the eastern valleys of Alpes-Maritimes in France and the Genoa basin in Italy. Rain amounting to several hundred millimeters was measured in the catchments of the Tinée River, the Vésubie, and the Roya: for example, 663 mm at the Mesches dam and 580 mm near the Tende Pass (Carrega and Michelot, 2021). These rivers experienced very high discharge floods, in terms of both peak flow (CEREMA, 2021; Payrastre et al., 2022) and intensity of sediment transport and the resulting morphological effects (Chmiel et al., 2022). This all resulted in ten deaths and eight missing persons as well as massive damage, to both buildings and linear infrastructure (roads, bridges, railways) concentrated in the valley floors (Carrega and Michelot, 2021; Rey et al., 2022). The French state launched two initiatives in the days following the event: (i) an emergency survey by the IGN (Institut Géographique National: French geographic survey) was conducted very rapidly, providing aerial orthophotos and a LiDAR (light detection and ranging) survey covering all of the main valleys in the impacted zone, and (ii) a broad back analysis was launched to mobilize technical actors and draw lessons from this extraordinary episode (ONF-RTM et al., 2022a). An analysis of the processes and geomorphological effects of the flooding was requested. It rapidly became evident that a great number

of bridges were destroyed and that the wood jams formed by large wood aggravated the phenomenon (SMIAGE, 2021). Since the event, almost every wood jams were removed from the river in the following months.

The Roya catchment has been strongly hit by this extreme event. The course of the Roya River is divided between France, where it rises at Tende Pass (1871 m), and Italy where it flows into the Mediterranean Sea at Ventimiglia (Figure 1). This catchment spreads over 394 km^2 in the French part (river length of 44 km); the whole drainage area at the sea is 660 km^2 (river length of 60 km). The Roya and its tributaries flow in rather narrow valleys confined by steep hillslopes. A few glacial basins, however, contain valleys that are slightly wider than the steep-sided gorge sections that separate these basins. The slope of the main channel is for the most part steep: it is greater than 5% in the uppermost part of the Roya's course, upstream of Viévola; it varies between 1.3% and 5.1% over 20 km located between Viévola and the confluence with the Caïros River and varies between 1% and 2% on the downstream 20 km located before the border (ONF-RTM et al., 2022a, p. 123). These steep slopes explain the rapid propagation of the floods, most particularly in the upper valley (BRGM-SCP, 2006). The streambeds of the Roya catchment are characterized by the presence of many very large boulders, a legacy of the successive Quaternary glacial periods; some of them also come from direct supplies from the rocky cliffs close to the streambeds.

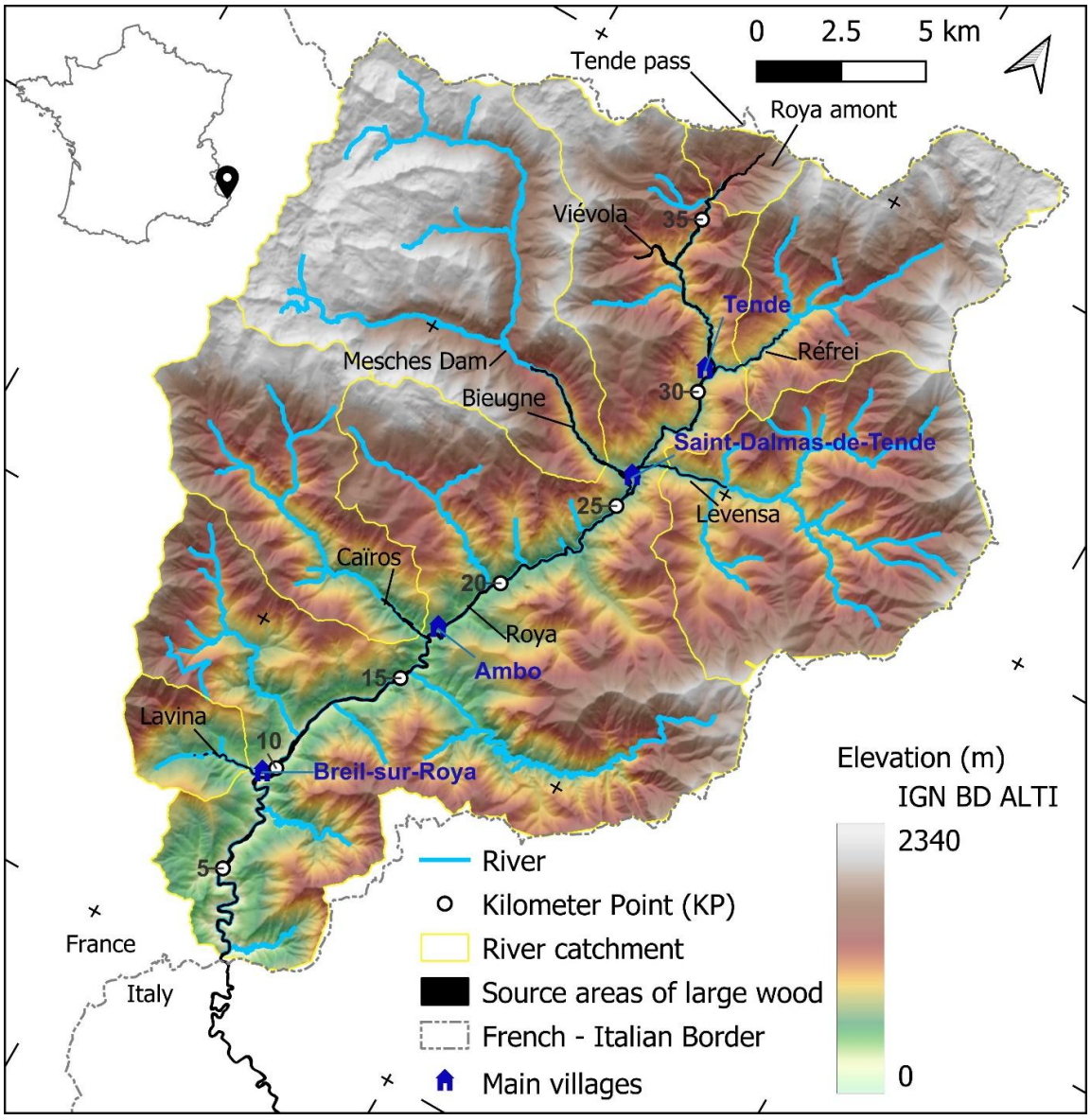

Figure 1: General map of the Roya River catchment and sub-catchments. The distances along the river given as kilometre point were measured along the valley axis (background elevation map from IGN BD (base de donnée: data base) ALTI - 25 m resolution).

2.2 GIS data used

Table 1 lists the GIS data used in the analysis. The following section gives a few details on their resolution, purpose, and source details.

Table 1 : Main GIS data used in the analysis (BD: base de donnée, i.e. data base; IFN: Inventaire Forestier National, i.e. French national forestry inventory, NDVI: Normalized Difference Vegetation Index)

Name (producer)	Nature (resolution)	Aim	Date of acquisition and access to the data
BD Foret V2 (IGN)	Polygons of forest (area>0.5 ha)	To map wooded area in the floodplain	Processed on 2014, available at https://geoservices.ign.fr/bdforet (accessed 09/06/2022)
IFN (IGN)	Statistics of forest plots unevenly distributed	To define forest density (tree/ha and m3/ha)	Campaigns from 2005 to 2018, available at https://inventaire-forestier.ign.fr/spip.php?rubrique159 (accessed 16/09/2020).
Sylvo Eco Region SER (IGN)	Polygon with associated note describing the main features of the SER	To select homogeneous forest regions in the IFN based on descriptions of the three local SER	H41 – Mid-southern Alps forest ecoregions (see https://inventaire-forestier.ign.fr/IMG/pdf/H_41.pdf), H42 – Southern internal Alps (see https://inventaire-forestier.ign.fr/IMG/pdf/H_42.pdf), J24 – Nice and pre-Ligurian areas (see https://inventaire-forestier.ign.fr/IMG/pdf/J24.pdf, (all accessed on 07/27/2023)
NDVI (European Space Agency)	Raster (pixel size: 8.5 m)	To compare biomass on hillslopes and in the floodplain	Picture acquired on 31 July and 28 September 2020 and after the storm (12 October 2020), available at https://earth.esa.int/eogateway/missions/planetscope (accessed 12/01/2022)
Orthophoto 2017 (IGN)	Raster (pixel size: 0.5m)	To map active channel before the flood	Pictures taken on 06/13/2017 – 07/06/2017, available at https://geoservices.ign.fr/bdortho (accessed 09/06/2022)
Orthophoto 2020 (IGN)	Raster (pixel size: 0.1m)	To map active channel after the flood	Data acquired on 03 & 04/10/2020, available at https://geoservices.ign.fr/ (accessed 09/06/2022)
LiDAR 2020 (IGN)	Point cloud (~10 pt/m²)	To compute height of riparian trees and map valley bottom	
the Sentinel-2 L2A (European Space Agency)	Raster (pixel size: 7.2 m)	To look for large wood ashore	Picture acquired on 3 October at 10:28, available on the Sentinel Hub EO Browser; http://apps.sentinel-hub.com/eo-browser/ (accessed 07/27/2022)

2.2.1 Forestry data

Two data sets were used primarily to define the extents of the wooded zones and the densities of the Roya's riparian tree stands:

- The IGN's BD Forêt V2 database provides polygons of wooded areas for all of France. Based on photo-interpretation of infrared images, it attributes to each polygon a type of vegetation class using a national nomenclature comprising 32 forest types that distinguish pure stands of the main forest species.
- The IFN (National Forest Inventory) provides, at the scale of plots scattered over the entire national territory, detailed forestry data. In every plot, each tree is inventoried (species, trunk diameter and height), the density of the stands is estimated (number of various type and size of trees/ha), as well as a great deal of site information (geomorphology, pedology, botany and proximity of the plot to a waterbody).

2.2.2 Remote sensing data

IGN orthophotos were used to digitize the active channels. The 2017 campaign was used to define the initial state (pre-event). The emergency survey after the Storm Alex was used to define the post-flooding state. This emergency survey only investigated the French course of the Roya River; therefore, the present analysis could only be carried out on this portion. For the sake of conciseness, it is understood throughout the article that the Roya's main stem or catchment designates the French part.

The Roya catchment was unfortunately not covered by a LiDAR survey of the overall area before the flooding. The IGN's emergency LiDAR survey provides, however, a detailed survey of the state of the geomorphology and the vegetation after the event. The pre-flooding topography of the streams in this valley are therefore only known through national and international low-resolution databases, which imposed strict limits on our ability to analyze the volumetric erosion and deposition assessments. However, post-flooding LiDAR imaging and orthophotos proved very useful in mapping the post-flooding residual vegetation and the valley floor defined here as the extent of historical alluvial deposits.

Satellite data were also used to verify whether the characteristics of the vegetation on the slopes observable after flooding could be applied to describe the height and volume of vegetation carried away by the flood. The Normalized Difference Vegetation Index (NDVI) was calculated at each dates from the reflectance value of the red and near infrared bands (NDVI=(NIR-Red)/(NIR+Red)) where NDVI is the normalized difference vegetation index, NIR and Red are spectral radiance or reflectance measurements recorded with sensors in NIR and red (visible) regions, respectively (Kriegler et al., 1969). The objective was to characterize the forest biomass along the river corridor and the slopes before the storm. The comparison between these two data series contributes to estimating the uncertainties of the model based on forest plots located on hillslopes (see Discussion).

2.3 Method used to estimate large wood supply

Large wood supply was estimated by multiplying the areas of the zones contributing to this supply by the density of the stands (trees/ha or m^3/ha). The methods used to estimate these two parameters are described in the following two subsections.

2.3.1 Selection of the contributing zones

The entire length of the Roya and its six tributaries had undergone geomorphological changes that were visible on the orthophotos in the emergency survey (Lavina, Caïros, Bieugne, Lévensa, Réfrei, and the Morte River at Viévola, see Figure 1). The upper catchment of the Roya upstream of the Viévola gorges (KP 36.8), with a catchment area of ~6 km^2, was also counted as a tributary of the main stem of the river and named "Roya amont" (upstream Roya).

The post-flood active channels were digitized manually. The active channel is defined as the area occupied by low-flow channels, unvegetated gravel bars, and gravel bars occupied by sparse vegetation (Williams and Rust, 1969; Bravard and Petit, 1997). The wooded islands were digitized independently and their area was excluded from active channel polygons. Generally speaking, the tributaries were very narrow before the flooding: their channel was distinguished only sporadically under the vegetation cover. Therefore, the choice was made not to digitize the active channels prior to flooding for these tributaries. The uncertainties of the assessment associated with this assumption, namely assuming that the initial width of the channels was negligible, are discussed in Section S3, as are the uncertainties associated with other possible contributing zones (upper catchments, landslides, and secondary ravines).

2.3.2 Estimation of surface areas contributing to large wood

The area of the zones that contributed to the supplies of large wood was estimated using the intersection of the polygons of the streams' active channels and the polygons of the wooded formations from the Forêt V2 database. The "Moors and heathlands" ("Landes") and "Grasslands" ("Formations herbacées)" polygons were removed after visually verifying that there were no forests in these two areas. Finally, a complete manual verification was done on the intersections, allowing us to remove from the assessment those polygons that actually showed no forests on the aerial photos. These artifacts were associated with imprecisions in the Forêt V2 database, which mapped continuous forest at the narrow gorges of the Roya. When the streambed was sufficiently wide, typically >15–20 m, the Forêt V2 database clearly demonstrated a gap or discontinuity and a non-wooded band at the river site. For streams so narrow that the majority of their width is hidden by the canopy, the method is less accurate (see Discussion).

2.3.3 Estimation of the stand densities

The IFN data are collected at the plot scale. To analyze the forest data in areas relatively similar to the catchment's forest, we extracted data of several SER (Sylvo Eco Region): (i) H41 – Mid-southern Alps forest ecoregions, which include the majority of the Roya and the Vésubie, but also (ii) H42 – Southern internal Alps and (iii) J24 – Nice and pre-Ligurian areas which incorporate the plots located on the neighboring slopes of the Tinée and Bévéra catchments. Only the most recent measurement was selected for those plots surveyed several times during the available period (2005 – 2018). The plots are located for the most part on slopes and unfortunately not on the valley floor. Their statistical representativeness for characterizing the forest stands at the valley bottom recruited by the flooding, i.e. alluvial forests rather than hillslope forests, is discussed in Section 4.1.

The number of stems per hectare and the volume of standing timber were assessed based on the characteristics of the trees and their weighting coefficient representing the number of tree equivalents per hectare of forest. To evaluate the timber volume, the IFN provides the volumes of "strong wood", i.e. only the trunk volume without the branches. We thus rather computed each tree volume using the EMERGE formula because it takes into account not only the volume of the trunk but also the volume of the main branches (Deleuze et al., 2014):

$$V_{tree} = \frac{h_{tot} \cdot \pi \cdot D_{BH}}{4\,\pi\left(1-\frac{1.3}{h_{tot}}\right)^2}\left(a_i + b_i \frac{\sqrt{\pi \cdot D_{BH}}}{h_{tot}} + c_i \frac{h_{tot}}{D_{BH}}\right) \quad (1)$$

where V_{tree} is the volume of large wood within the tree [m³], h_{tot} is the total height of the tree [m], D_{BH} is the diameter of the tree at breast height (1.3 m) and a_i, b_i and c_i are three shape coefficients for which generic values exist for deciduous and coniferous (a_i = 0.522 , b_i = 0.661, c_i = -0.002, and a_i = 0.356 , b_i = 1.756, c_i = 0.002, respectively), but species-specific values provided in Table S1 also exist and were used whenever possible.

The post-flooding LiDAR data were also analyzed using automatic tree detection scripts to describe the active channel zones where trees had survived as well as the height of trees in the residual riparian trees of the Roya and its tributaries. The R library, "LidaRtRee" from Monnet (2020), was used; its validation is provided in Eysn et al. (2015).

2.4 Large wood deposit estimation method

The particularly fine resolution of the IGN emergency orthophotos (10 cm resolution) made it possible to manually digitize as polylines the trunks and branches of the trees deposited in the active channels. Resolution coarser than 0.1 would probably make the work much more uncertain and subjective. Figure 2 illustrates the digitization work at a scale close to that used for digitization. It should be noted that the digitization work focused on the large wood transported by the flood. The deposits of windfall, i.e., dead wood located within the other processes resulting in entrainment of fresh wood or dead wood, notably on slopes (e.g., landslide processes), were not included in the digitization so that the deposits on forest slopes would not be taken into account.

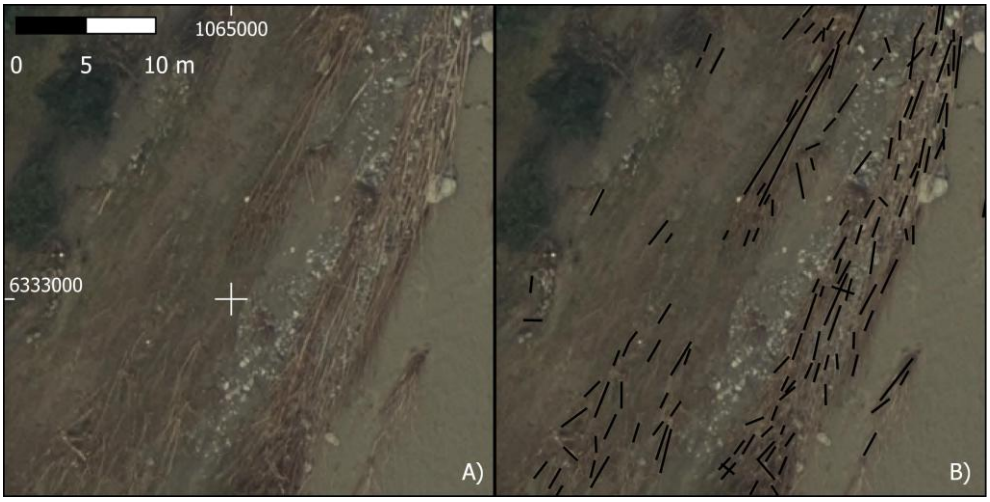

Figure 2 : **Examples of deposits of large wood on the emergency aerial survey near Fontan village: A) raw image, and B) example of digitized large wood deposits. The coordinate system used is the Lambert93 system (EPSG 2154)**

The image resolution was however too limited for a systematic measurement of the diameters of the large wood. This datum is nonetheless necessary to estimate the volume of large wood deposited (V_{lw}) by hypothesizing that these were cylindrical trunks:

$$V_{lw} = L \cdot D^2 \cdot \frac{\pi}{4} \quad (2)$$

with L the length of large wood measured by digitization (m), D their diameter (m), and V_{lw} their solid volume (m³). It should be noted that the vast majority of the large wood digitized is without branches and roots and that this assumption is generally valid.

A sample of 54 wood pieces was randomly selected in the digitized large wood. Their diameter was digitized at the ends and the center so as to estimate the robustness of the diameter measurement, which is by nature imprecise given the resolution of the source images (0.10 m). The mean value of measured diameters is 0.18 m and varies from 0.11 to 0.30 m ± 0.04 m, depending on whether the middle or the ends were considered. These values are most probably quite accurate but do not include the diameters of a few much larger key pieces. Among those pieces found on the site during the field visit in October 2021, 1 year after the storm (see Section S2), the center diameters of ten pieces measured provided an equivalent order of magnitude (mean, 0.15 m; range, 0.02–0.29 m). Near the stumps, the diameters sometimes reached 0.5 m, but rarely is the entire trunk so large. To provide an order of magnitude of the mean diameter applied to all the digitized wood pieces to calculate the volumes of deposited wood, the mean value of the mean diameters (0.18 m) was used, with additional calculations of the high and low values of 0.3 m and 0.1 m, respectively, to provide an uncertainty range.

2.5 Segmentation of the study zone and statistical analysis

To conduct a longitudinal analysis, the stream was segmented, as in classic river geomorphology and longitudinal analyses (Roux et al., 2015). This segmentation followed the classic steps: (i) verification of the polygon delineating the valley floor, (ii) extraction of the polygon's axis, with manual verification and correction if necessary, (iii) plot of the transects orthogonal to the axis, regularly spaced (200 m), with manual verification and correction if need be, and (iv) definition of 200 m-long valley floor reaches based on these transects. Valley floor polygons identified by their Kilometers point (KP) estimated on the axis of the valley from the Italy-France border were thus available to estimate the longitudinal evolution of the different parameters on each river reach. A statistical analysis was conducted on all of these reach parameters to determine the Spearman correlations and the coefficients of determination linking them.

3 Results

3.1 Analysis of source zones

3.1.1 Analysis of the contributing surface areas

Of the 251.5 ha of valley floor of the Roya and its tributaries, 133 ha were covered before the flooding by riparian trees distributed relatively evenly throughout the linear zone studied. More than half was lost during the flood. Bank erosion processes that affected the main streambed of the Roya between KP 0 and 36.7 transformed its active channel from 58.5 ha to 136.0 ha, increasing it by a factor of 2.33. The mean width changed from 16 m to 37 m (Melun et al., 2022).

Overlaying and comparing the active channel with the Forêt V2 database resulted in an estimated 48.3 ha of eroded wooded area on the main stem of the Roya and 38.5 ha on its tributaries – 10.7 ha for the Bieugne and 12.4 ha for the Caïros – for a total of 86.78 ha (Table 2). The mean canopy cover rate in the segments decreased from 57 to 20%. As mentioned above, the GIS layer created does not include the pre-flood active channel of the tributaries. It should be noted that during the manual verification stage, 21.1 ha were removed from the actual existing wooded area in the intersection of the Forêt V2 database and the pre-flood active channel on the main stem of the Roya.

Table 2 : Parameters describing the geomorphology, supply, and deposition of large wood in the water courses of the Roya catchment

River	KP of the confluence from the French border	Valley length of the active area (L)	Area of the active width *post*-event (S)	Mean active width (S/L)	Large wood pieces digitized (N_{lw})	Length of large wood digitized (L_{lw})	Linear density of large wood (N_{lw}/L)	Surface density of large wood (N_{lw}/S)	Area of eroded wood (BD Forêt V2)
Units	[km]	[m]	[m²]	[m]	[pieces]	[m]	[pieces/km]	[pieces/ha]	[m²]
Roya	-	36,786	1,360,300 (584,629)†	37.0	12,360	24,718	336	91	482,915
Roya amont	36.7	1,477	54,468	37.8	917	1,694	636	168	54,334
Viévola	34.8	1,690	83,744	49.6	718	1,692	425	86	36,351
Réfrei	30.8	2,928	47,193	16.1	635	867	217	135	32,174
Lévensa	26.4	2,768	54,300	19.6	332	513	120	61	21,657
Bieugne	25.6	5,438	203,826	37.5	926	1,853	170	45	107,060
Caïros	17.2	1,807 (6,107‡)	59,356 (154,007‡)	32.8 (25.2‡)	612 (1,588‡)	1 034 (2,683‡)	339 (260‡)	103 (103‡)	47,726 (123,831)‡
Lavina	9.3	2,372	26,692	11.3	346	465	146	130	9,471
Total	-	59,530	1,984 530	33.3	16,846	34,389	200	90	867,792‡

†Area *ante*-event. ‡Value corrected using drone images, see Supplement S3.

3.1.2 Analysis of the stand densities

To estimate the stand densities, the low, intermediate, and high stand density values, defined as the three quartiles of the distributions studied, were extracted from three subsamples of the IFN database : (i) 128 plots were taken from SER H41 only, (ii) 208 plots were selected because located in the Tinée, Vésubie, Bévéra, and Roya catchments, and (iii) 57 plots were selected because located in the Roya catchment. The volumes of wood per hectare of these three subsamples are quite similar (Table 3). We retained the second sample, whose size is four times greater than the strict Roya sample, but which has the advantage of being located on or near the study zone (SER H41 extends more toward the north). Hillslope forests of this zone present a certain variability in stand density and standing tree volume (Figure 3). This is true for both the plots whose proximity to the hydrographic network is unknown (light yellow) and those possibly representative of riparian forests because they are located near a stream or a water source (red or purple). It can also be seen that a large majority of the plots whose location in relation to the local hydrography is known (this parameter has only been surveyed since 2013) are classified as "0, No hydrography" (grey) and therefore are not riparian trees *stricto sensu*. None of the plots belongs to classes 5 and 6, associated with rivers. This is symptomatic of the lack of IFN observations in riparian formations.

Table 3 : Forest density data used for the analysis

Parameter	Area of estimation	n (plot)	Estimations		
			Low (quantile 25 %)	Intermediate (median)	High (quantile 75 %)
Trees per hectare [tree/ha]	SER H41	128	337	628	885
	Tinée, Vésubie, Bevera, Roya	208	242	560	905
	Roya	57	305	626	904
Volume of wood per hectare [m³/ha]	SER H41	128	92	208	343
	Tinée, Vésubie, Bevera, Roya	208	89	168	342
	Roya	57	90	174	349

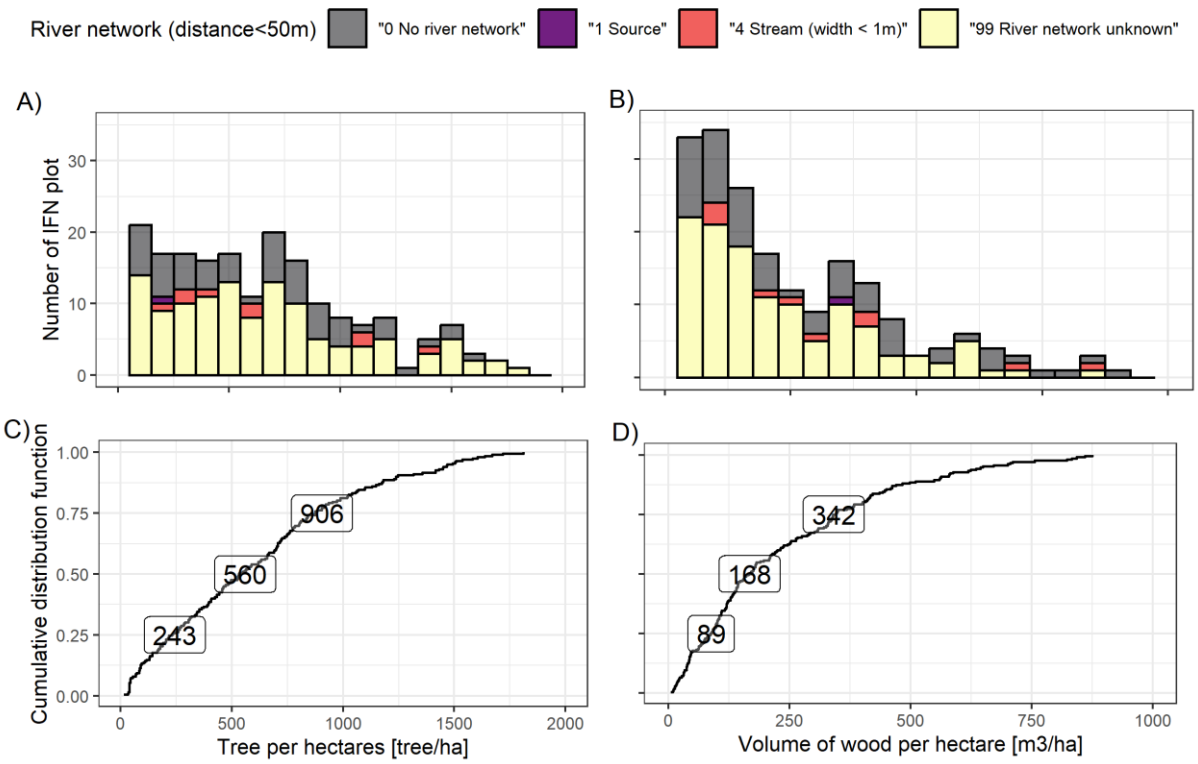

Figure 3 : Forest statistics of the 208 single plots used in the analysis: A) histogram of number of trees per hectare, B) histogram of large wood volume per hectare with a color code depending on the distance from the plot to the river network, C) quantiles of number of trees per hectare, and D) quantiles of large wood volume per hectare. Number in squares are quartiles.

3.2 Analysis of deposits

The large wood deposits were manually digitized as polylines over 54.8 km within the Roya catchment: 36.8 km of the main stem and 18.5 km of the tributaries. A total of 16,846 independent pieces forming a cumulative length of 32.83 km of trunks and branches were identified (Table 2). Taking into account the river length or the surface area of the active channel, the upstream Roya and the Viévola rivers were the largest deposition sites of large wood. They deposited 1,147 m and 975 m of large wood per kilometer of stream, respectively. These sections are located north of the catchment, where the Roya presents the steepest slopes. These sectors are also near the sites of the maximum rainfall measurement recorded during the event (Carrega and Michelot, 2021). Both factors probably contributed to the high recruitment of large wood. These elements maybe less transported further downstream because the channel width of these headwaters are narrower than further downstream. The less active tributaries (Caïros, Lévensa, Lavina, and Réfrei) showed rates of large wood deposition between 167 and 298 m/km. The two main branches, the Roya and the Bieugne, had values of 672 and 378 m/km, respectively. In most of the sectors, the number of large wood pieces deposited was less than 200 pieces/km. Some sectors were more heavily loaded, e.g., more than 600 pieces/km in the upstream Roya. The cumulative number and length of large wood pieces compared to the surface area of the active channel after the flood ranged from 50 to 100 pieces/ha and from 75 to 200 m of large wood/ha. On average, the deposits were on the order of 4 m^3/ha of the post-flood active channel.

Crossing the polygons of the river sections with the centroids of the polylines representing the tree trunks deposited allows counting the large wood by 200-m long reaches. The number of large wood pieces deposited in each reach was compared to the width of the active channel in Figure 4. Data were widely scattered but the number of pieces deposited and their cumulative length seems to increase substantially with the active channel width (r^2 = 0.23 and 0.31, respectively, Spearman correlation). A better coefficient of determination was observed between the length or the number of large wood pieces and the valley's area (r^2=0.37 and 0.31 respectively, Spearman correlation).

We observed that very few sections less than 10–20 m wide had stored more than 50 pieces: narrow sectors are not suitable to large wood deposition. This trend is most probably related to the acceleration of flows in these sections and the lack of gravel bars and islands prone to trap large wood. In contrast, deposits increased (>150–200 elements) in the wide active channels (width >50 m). Sections of the tributaries >70 m wide coincided with zones of massive sediment deposits on the alluvial fan of the tributaries: the number of pieces identified was lower than on sections of the Roya with the same width. Large wood may more often be buried in these landforms. Further research will be necessary to assess these volumes, which were not explored in the present study. It should also be mentioned that the emergency spillways of the Mesches dam was heavily submerged during the flood; therefore, large wood did not accumulate here, in contrast to bridges, which acted as obstacles (SMIAGE, 2021), e.g. at Breil-sur-Roya where about 500 to 1,000 m^3 of large wood and debris accumulative in the lake upstream of the bridges and hydraulic structures (personal communication with M. Giordan).

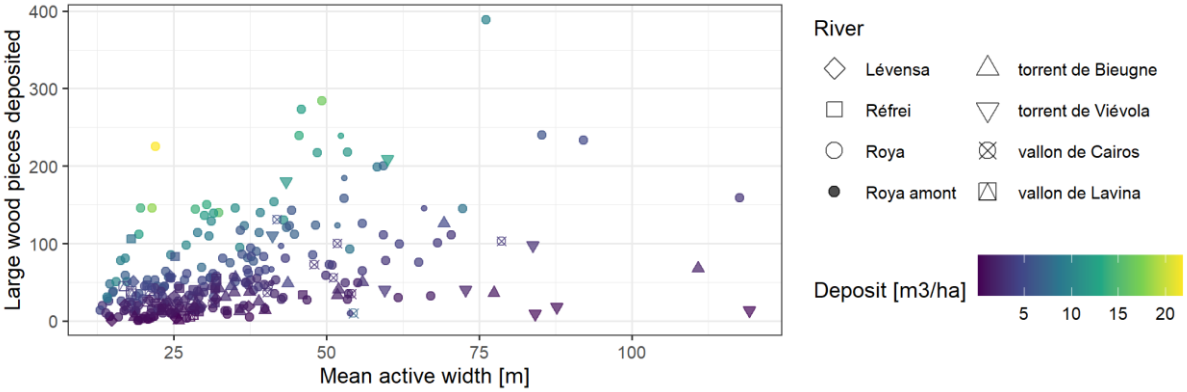

Figure 4 : **Number of large wood pieces versus active channel width computed on 200-m long reaches**

3.3 Volumetric assessment of large wood of the French Roya

All of the estimations presented above provide information for a longitudinal assessment of the sources and deposits in relation to the KP (Figure 5, see also Appendix 18 of ONF-RTM et al., 2022a). Wood inputs in volume from the seven active tributaries were introduced at the confluence KPs. The values of the tributary supplies were significant compared to the volumes mobilized in the 200-m reaches of the main stem. These values, too high to appear on the graph, are provided in Table 4. The locally high supplies generated sudden rises in the assessment presented in Figure 5D. Figure 5A shows the order of magnitude of the surface areas of the pre- and post-flood active channel by 200-m reaches. The rocky gorges, downstream from Saint-Dalmas-de-Tende, Ambo and Breil-sur-Roya, stand out for their lower widening rates. The upstream reaches underwent the strongest active channel growth and the greatest mean supply of large wood for the reasons discussed in Section 3.3 (Figure 5B and 5C).

Figure 5B illustrates the estimated number of trees recruited and the number of large wood pieces deposited. High or low homogenous recruitment sectors can also be seen; they are directly associated with more or less pronounced widening of the active channel. The very pronounced widening at Breil-sur-Roya did not, however, supply as much large wood because the land near the active channel was less dominated by wooded zones. It can also be seen that the number of pieces deposited was significantly lower than the number of trees potentially recruited. In addition, it should be noted that a recruited tree necessarily supplies several large wood pieces because of the mechanical breakage phenomenon studied through the reduction rate in the following section.

Figure 5C presents the assessment of the volume of wood that was uprooted and deposited, including the uncertainty associated with the assumption of large wood diameters. Here again, the volumes deposited, even though *very locally* surpassing 50 m^3 per 200-m section, are marginal compared to the volumes recruited that *regularly* surpass 100 m^3 per section.

Figure 5D provides the cumulative assessment with propagation of uncertainties from upstream to downstream. The estimations are globally increasing, demonstrating that, whatever assumption is applied (high, low, or intermediate), the volumes deposited are systematically lower than the volumes

eroded. The overall assessment concludes in a net export on the order of 14,000 m³ of large wood with uncertainty ranging from 5,000 to 29,500 m³.

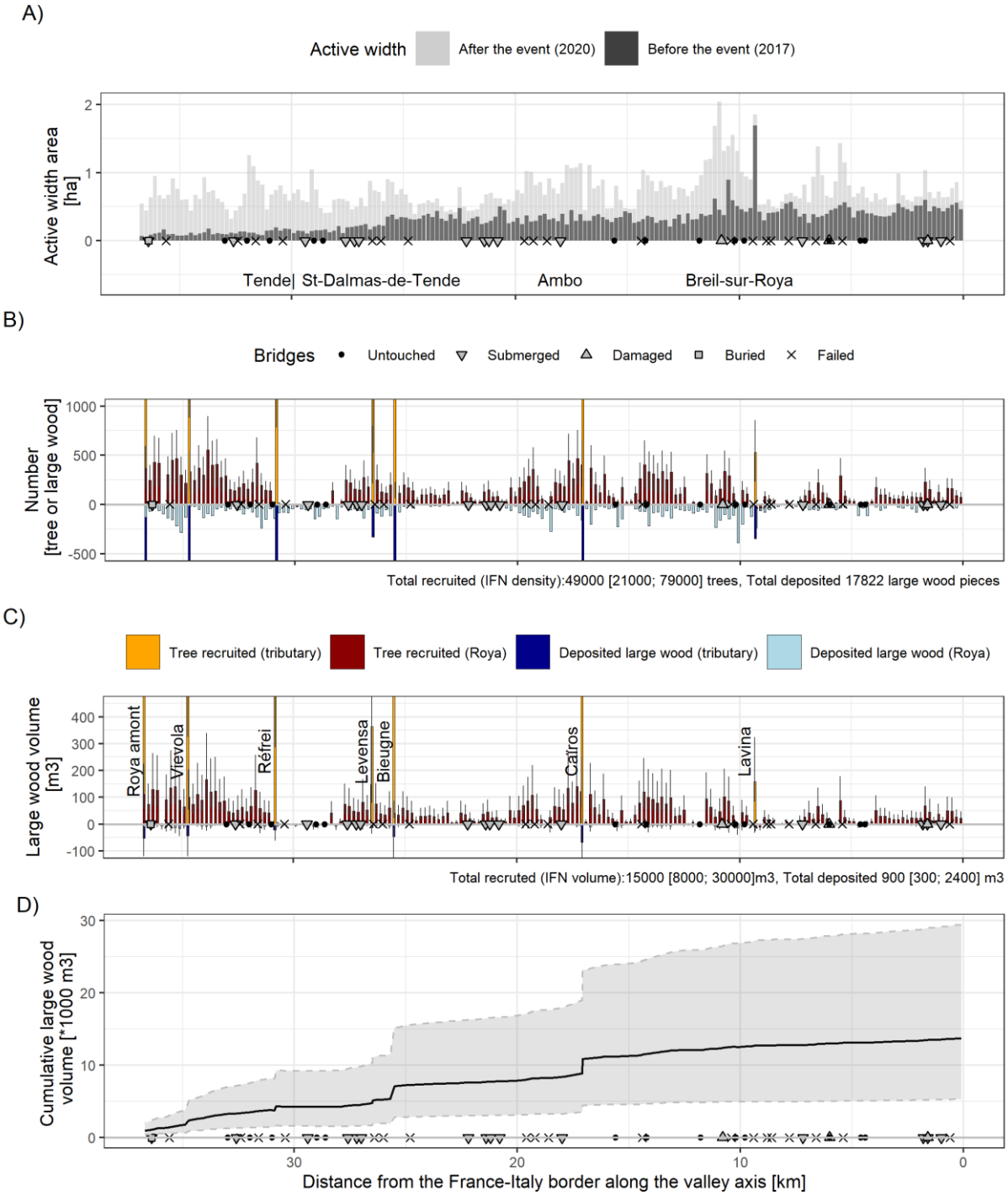

Figure 5 : Longitudinal analysis of the Roya River main stem: A) Evolution of the active width; B) Number of recruited trees and number of deposited pieces; C) Volume of recruited and deposited large wood, and D) Cumulative volumetric assessment. The error bars and strips are estimated with the high and low envelopes of the estimates of the different assessments.

The relative contributions of the different compartments are detailed in Figure 6; the uncertainty ranges are presented in Table 4. Insofar as the supply was systematically greater than the deposits, the balance is dominated by the main supply sources. The tributaries of the Roya therefore typically supplied large wood on the order of 1000 m³ (e.g., upstream Roya, the Morte River at Viévola or Réfrei). The Levensa and the Lavina are considered slightly less productive (a few hundred m³) and the Bieugne and Caïros rivers more productive (several thousand m³). The main net supplier of large wood is therefore

considered as being the main stem of the Roya (55% of exports, i.e., supplies minus deposits), with the tributaries supplying the rest (45%). These respective contributions are coherent with the linear stretches of zones that were very active morphologically: 36.7 km on the Roya and 22.0 km on the tributaries: 60% and 40%, respectively, of the total linear river at the scale of the French catchment.

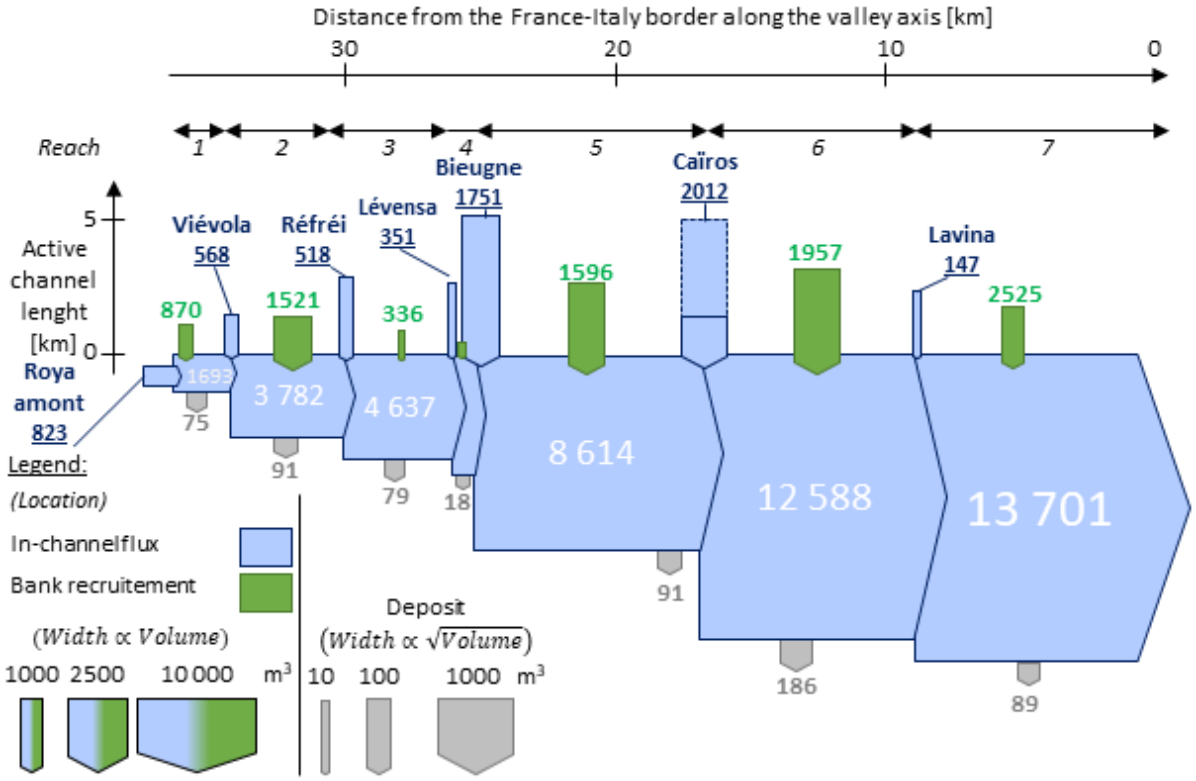

Figure 6: Synthesis plot of the large wood volumes supplied and transferred within the French Roya catchment during the Storm Alex. The numbers displayed correspond to the intermediate estimations. Blue blocks represent fluxes in the various channel, green blocks the input from bank erosions, grey blocks the loss through deposition. Block width is volume dependent and length is channel-length dependent.

Table 4 : Large wood volume eroded, deposited, supplied and cumulative in the sub-catchments and intermediate reaches: mid value (lower range – upper range)

Reach	Recruited volume [m³]	Deposited volume[m³]	Input [m³]	Cumulative sum [m³]
-Roya Amont	913 (484 – 1,858)	43(13 - 120)	870 (364 – 1,845)	870 (364 – 1,845)
Roya (Reach 1)	898 (476 – 1,828)	75 (23 - 208)	823 (268 – 1,805)	1,693 (632 – 3,650)
- Viévola	611 (324 – 1,243)	43 (13 - 120)	568 (204 – 1,230)	2,319 (853 – 5,010)
Roya (Reach 2)	1,613 (854 – 3,283)	91 (28 - 254)	1,521 (600 – 3,254)	3,782 (1,437 – 8,134)
- Réfrei	541 (286 – 1,100)	22 (7 - 61)	518 (225 – 1,094)	4,300 (1,662 – 9,228)
Roya (Reach 3)	415 (220 - 845)	79 (24 - 219)	336 (116 - 820)	4,637 (1,663 – 10,048)
- Lévensa	364 (193 - 741)	13 (4 - 36)	351 (157 - 737)	4,987 (1,819 – 10,785)
Roya (Reach 4)	297 (157 - 604)	18 (5 - 49)	279 (108 - 599)	5,266 (1,928 – 11,383)
- Bieugne	1,799 (953 – 3,661)	47 (15 - 131)	1,751 (822 – 3,647)	7,072 (2,764 – 15,151)
Roya (Reach 5)	1,687 (894 – 3,435)	91 (28 - 254)	1,596 (640 – 3,407)	8,614 (3,390 – 18,437)
-Caïros	2,080 (1,102 – 4,235)	68 (21 - 190)	2,012 (912 – 4,214)	10,762 (4,363 – 22,936)
Roya (Tronçon 6)	2,143 (1,135 – 4,362)	186 (57 - 517)	1,957 (619 – 4,305)	12,588 (4,964 – 26,958)
-Lavina	159 (84 - 324)	12 (4 - 33)	147 (51.4 - 320)	12,730 (4,972 – 27,277)
Roya (Tronçon 7)	1,060 (562 – 2,159)	89 (28 - 248)	971 (314 – 2,131)	13,701 (5,286 – 29,408)
Total	14,580 (7,724 – 29,678)	878 (271 – 2,440)	13,701 (5,286 – 29,408)	13,701 (5,286 – 29,408)

3.4 Analysis of the size of large wood pieces

3.4.1 Large wood length

Digitization of this type of large wood sample also makes it possible to examine the size of the pieces. Table 5 a compilation of quantiles for various samples is presented for all of the trees inventoried (the Roya and its tributaries). The large wood for the most part comprises short pieces (median length, 1.4 m; 75% of the pieces <2.1 m). Only 10% of the large wood pieces are longer than 3.6 m, 5% longer than 5.2 m, and 1% longer than 10 m. These key pieces are a minority within a multitude: although they make up only 1% of the sample, more than 150 were counted. These are, essentially, the pieces that were found in the field during the October 2021 mission (mean length, 11.2 m, 76% of the trunks were more than 10 m long). This result testifies to the violence with which the large wood was transported and shattered, taking into account the hardness of the wood of the dominating species (*Ostrya carpinifolia* and *Fraxinus excelsior*), in contrast to the soft wood species generally observed in riparian trees (Piégay et al., 1994).

Table 5 : Quantiles of standing tree height, diameter and length of large wood pieces predicted and measured

Parameter	Source	Quantile						
		0%	25%	50%	75%	90%	95%	99%
Stand tree height (m)	LiDAR	5.0	8.9	13.0	17.5	21.5	24.4	30
Length of large wood pieces (m): measured	Digitized	1.0	1.0	1.4	2.1	3.6	5.2	10.3
Length of large wood pieces (m): predicted	Monte Carlo approach, Quiniou et al., 2022	0.1	1.2	2.1	3.4	5.1	6.5	9.6

3.4.2 Rate of tree length reduction: theory and observations

With the distribution of large wood lengths measured (the uncertainties concerning these measurements are discussed in Section 4.1), it is interesting to compare these observations with the predictive methods used for this parameter. The probabilistic method reported by Quiniou et al. (2022) was used to predict the length of large wood based on the height of standing trees. This meant the length of large wood could be predicted by multiplying a coefficient of reduction (R) by the total tree height h_{tot}:

$$L_{lw} = R \cdot h_{tot} \quad (3)$$

This theoretical method is compared to the digitized tree measurements in Figure 7. The data used to draw Figure 7A were taken from a study conducted by Rickli et al. (2018) after the 2005 floods in Switzerland. The researchers measured the length and diameter of the large wood deposited in the field. Their approach makes it possible to reconstruct the height h_{tot} of the trees before they were broken up using forest data and models, i.e. the theoretical value is reconstructed. The rate of reduction R is thus deduced by the ratio L_{lw}/h_{tot}. The black solid line in Figure 7A represents the entire sample of wood pieces whose diameter was greater than 10 cm. The grey lines represent the subsamples associated with each of the rivers inventoried. They show the spatial variability of the coefficient of reduction R between the rivers. For information, the distribution of the R values estimated on the pieces with a diameter <0.1 m is represented by dotted lines.

It can be seen that the vast majority of the R values are <0.5 and the large majority <0.3, showing that most of the large wood pieces are significantly shorter than the length of the original trunk: the large wood is nearly systematically half as long as the standing tree, and for the most part three to five times shorter (i.e. R<0.2 – 0.3). These curves also demonstrate that a certain variability exists in the rate of reduction. It should be remembered that this is a rate of reduction evaluated on short steep creeks in Switzerland that are quite different from those examined within this study. The digitized data on the Roya were used to test their transferability.

Figure 7B is based on a comparison between the trees detected on LiDAR (dotted lines, one line per river: the Roya or the tributaries; the bright red line represents the entire sample). It can be noted that

the highest trees reached 30–40 m. To predict the length of the large wood using Equation (3) and based on these data and the reduction rate values in Figure 7A, a random selection using the Monte-Carlo approach was adopted according to the probabilistic approach proposed by Quiniou et al. (2022). The length of the large wood thus predicted is relatively short for the majority of the pieces (see Table 5: 1st quartile: 1.2 m; median: 2.1 m). According to the trajectory of this simulation curve (dashed grey lines), the majority of the large wood coming from riparian trees of the Roya catchment would have had lengths <10 m.

The red solid lines in Figure 7B correspond to the statistical distributions of the large wood measured on the Roya catchment and its tributaries. The overall form of the distribution is very similar to that predicted by the probabilistic approach. The comparison of the quantiles provided in Table 5 shows that the measurements are less than the probabilistic estimations; nonetheless, the order of magnitude remains satisfactory (Figure 7). The rate of reduction between the tree height and the length of large wood observed following the Storm Alex in the Roya catchment seems slightly higher than that observed on the small rivers in Switzerland by Rickli et al. (2018), but the order of magnitude and the distribution are, finally, quite similar. One can note that an opposite trend was detected on the Vésubie whose bed is wider and the geomorphology more braided in aspect (ONF-RTM et al., 2022b). The lower number of narrow gorges occupied by very large boulders forming obstacles against which the current projected the large wood pieces very likely explains this observation.

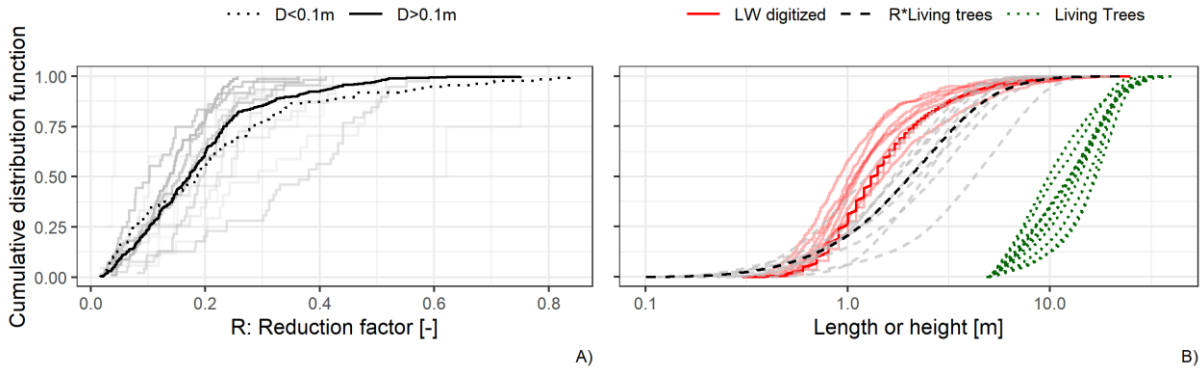

Figure 7: Statistical distributions of large wood reduction rate R estimated by Rickli et al. (2018); B) Statistical distributions of the height of standing trees detected (dotted green lines), of the large wood length predicted by probabilistic estimation (dashed grey lines) and measured by digitization (continuous red lines) in the Roya valley and its tributaries (one line per river)

4 Discussion

4.1 Analysis of the different sources of uncertainty

The approach developed in the present work consisted in completing an assessment integrating the main contributions to the supplies and deposits of large wood identified directly after the flooding event. It is based on photo-interpretation operations aiming to digitize the main contributing zones and the deposited large wood. It is simple to implement albeit fairly long if the studied reaches are long. In our application case, the estimations of recruited wood are much greater than those of large wood deposited along the streambeds. The three sections provided in the Supplemental Information address the potential causes of uncertainty. They rely on less rigorous approaches than the overall method or use data sources that are less accessible or more sophisticated. Such uncertainty estimations are not needed in applying the basic method such as presented above. These reflections simply aim to take a step back from the hypotheses that underlie the approach.

Table 6 summarizes the different sources of uncertainty and the relative uncertainty associated with the assessment. Quadratic propagation of the relative uncertainties, as is usually conducted in uncertainty propagation (JCGM, 2008), may not take into account the under- or overestimation identified and would result in a relative uncertainty of ±35%. However, the uncertainties associated with the contributions overlooked in the first approach are partially compensated and correspond to −15% uncertainty on the intermediate estimation of export in the assessment (13,701 m³). The assessment overestimated export by potentially 30%, as projected by the assumption of a minimum initial width of the tributaries. It

therefore seems that it is important to map the initial active channels, or at least roughly estimate their surface area and integrate this information into the assessment. At the same time, several of the catchment's supplying compartments were overlooked, with the small gullies and tributaries generating uncertainty on the order of 10% in the assessment. The whole of these uncertainties remains significantly lower than those provided in Table 4, which are strongly dominated by the poor knowledge of the riparian tree stand densities (values provided in Table 3).

Table 6 : Sources and potential values of uncertainties in the volume of large wood

Uncertainty source	Effect†	Crude estimation of the uncertainty Approach used	Value [m³]	Relative uncertainty
Neglected active width before the flood on tributaries	↗	Mean channel width measured on 5 profiles * tributary channel length (22.7 km) * 168 m³/ha	-4,050	-30 %
Neglected supply from landslides	↘	Geomorphical map crossed with the forest inventory BD Forêt V2	1,150	+8
Neglected supply from the small secondary tributaries	↘	Assumption of a channel width of 2 m * active channel length on the geomorphic survey + surface area of main active area on the geomorphic survey	1,650	+12 %
Ignored supply from the headwaters of the Bieugne (Casterino and Merveilles areas)	↗	Crossing of the forest inventory (BD Forêt V2) with the geomorphic survey * process-specific volume density (see Supplement S3)	750	+5 %
Neglected supply from the active width of the Caïros channel located outside the emergency IGN survey	Integrated in the assessment	Proportionally to the total active channel length estimated by drone images (see Supplement S3)	2,507	Integrated in the assessment
Ignored supply by the active width of the Levensa	↗	Arbitrarily estimated as equivalent to the mapped supply	450	+3 %
Bias related to the use of wood volume data measured on hillslope	↘	Overestimation of the riparian biomass estimated by remote sensing (see Supplement S2)	1,100	-8 %
Length of large wood invisible on the aerial survey	↘	Underestimation of the digitized length by 2 m (see Supplement S3)	-900	-7 %
Cumulative uncertainties			+4,000 -6,050	-15 %

† The sign ↘ means that the uncertainty source makes the assessment underestimated, while ↗ means that the uncertainty source make the assessment overestimated.

In sum, it seems that the uncertainties associated with an assessment such as the one conducted in this study could be reduced based on the following elements (in order of importance): (i) by improving our knowledge on the tree stand densities of the riparian forests, (ii) by integrating the initial channel widths, even those in the zones where the channels are covered by vegetation on aerial photos, and (iii) by integrating the contributing surface areas associated with the more scattered and extended processes such as small gullies and only partially active tributaries.

4.2 Comments on the downstream dynamics (Italian Roya and the Mediterranean Sea)

These volumes were exported toward Italy and then the Mediterranean Sea. We were not able to obtain information on the volumes of large wood evacuated from beaches and the banks of the Roya. Images acquired by the Italian Protezione Civile on the final section of the Roya and its estuary show deposits of large wood that are quite similar to those observed further upstream on the French Roya (Figure 8). Accumulations are present but of limited size, corresponding to volumes of a few tens of cubic meters

to a few hundred cubic meters, moreover largely made up of air (Livers et al., 2020), small wood pieces, and various types of debris. Wooded formations were also recruited in the 16 km of the Roya's Italian channel (Figure 8A). Therefore, the assessment on the Italian side is also most likely unbalanced toward a net export to the sea.

Figure 8: A) General map of the Roya catchment including the studied reaches and catchments (yellow) and the Italian downstream part; B) aerial picture of the Roya mouth into the Mediterranean sea (Source: google earth); C) same image in grey scale and location of the drone image; D - F) Drone images of 5 October 2020 from the Italian Roya to Ventimiglia (Source: Protezione Civile)

Large wood was therefore exported toward the sea. The Alpes-Maritimes maritime prefecture even prohibited navigation and sent two ships to retrieve some large wood pieces. These ships collected between 270 and 400 tons of wood, between Cap Ferrat and Dramont, up to 10 nautical miles offshore between 6 and 20 October 2020 (source: personal communications with the Alpes-Maritimes prefecture). On 3 October at 10:28, immediately after the flooding, the Sentinel-2 L2A satellite acquired an image of the zone (Table 1). The turbidity current associated with the flood clearly appears on this image (Figure 9A). A carpet of drifting large wood can be observed 19 km from the Roya estuary (Figure 9B). Approximately 5 km long, this carpet has a surface area exceeding 46 ha. The volume of the associated large wood can be very roughly estimated. Let us assume that it is formed of a single layer of large wood with a thickness on the order of the mean diameter of the large wood (0.18 m) and that this carpet has high porosity, on the order of 0.6–0.8, characteristic of fairly loose deposits (Livers et al., 2020). The volume of associated large wood could be on the order of 17,000–34,000 m^3, i.e., more than the intermediate export value estimated for the French Roya alone. This order of magnitude is coherent:

it certainly seems that the flooding associated with the Storm Alex exported massive quantities of large wood into the sea.

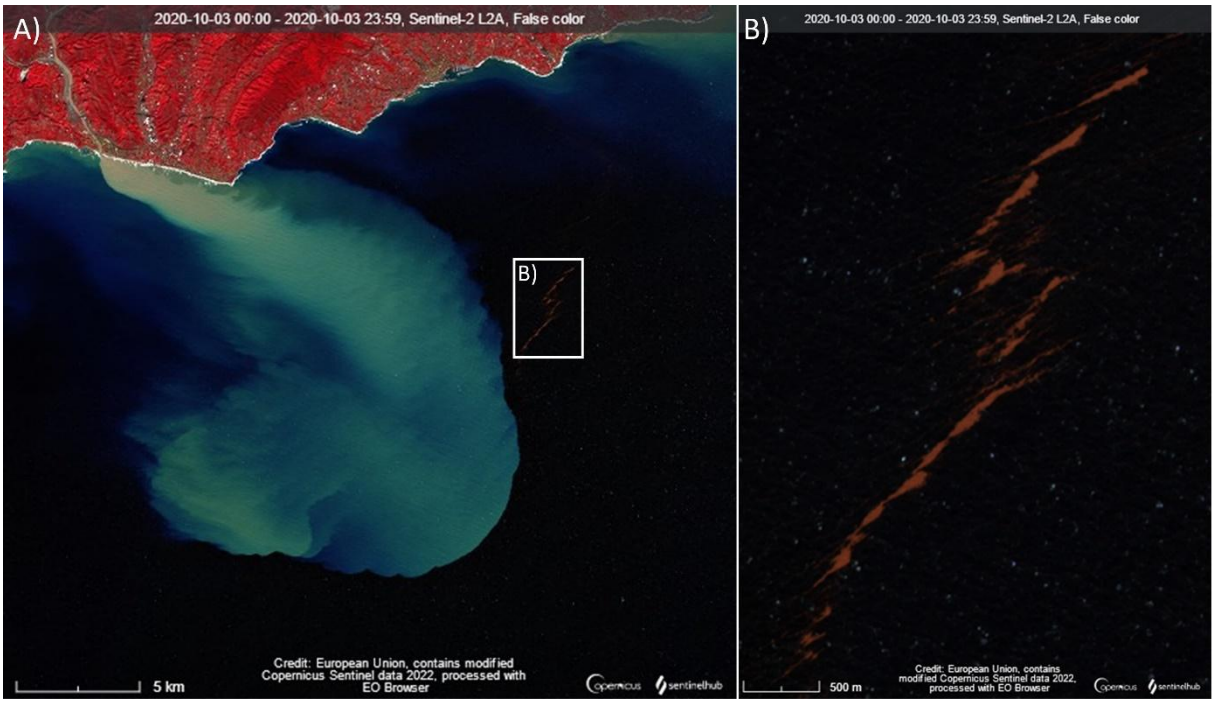

Figure 9: Sentinel-2 L2A satellite image of 3 October 10:28 showing: A) the turbidity current of the Roya outlet at sea and B) the large wood raft drifting offshore

4.3 Comparison with other rivers and floods

'The supply of large wood associated with Storm Alex in the Roya catchment is compared in Figure 10 with assessments of wood supply mobilized in other storm-impacted catchments in the Alps and Japan (Rickenmann, 1997; Schmocker and Weitbrecht, 2013; Steeb et al., 2017, 2023; Lucía et al., 2018). It can be clearly seen that the points raised by this study are comparable to the strongest values of the data available from other catchments of similar size. As in earlier studies, large wood supply varies in the catchment depending on the valley's geometry (width, succession of gorges and wider parts, and surface area and slope of valley floors), the location of rainfall maximums observed during the flood, and the extent of trees prior to the flood.

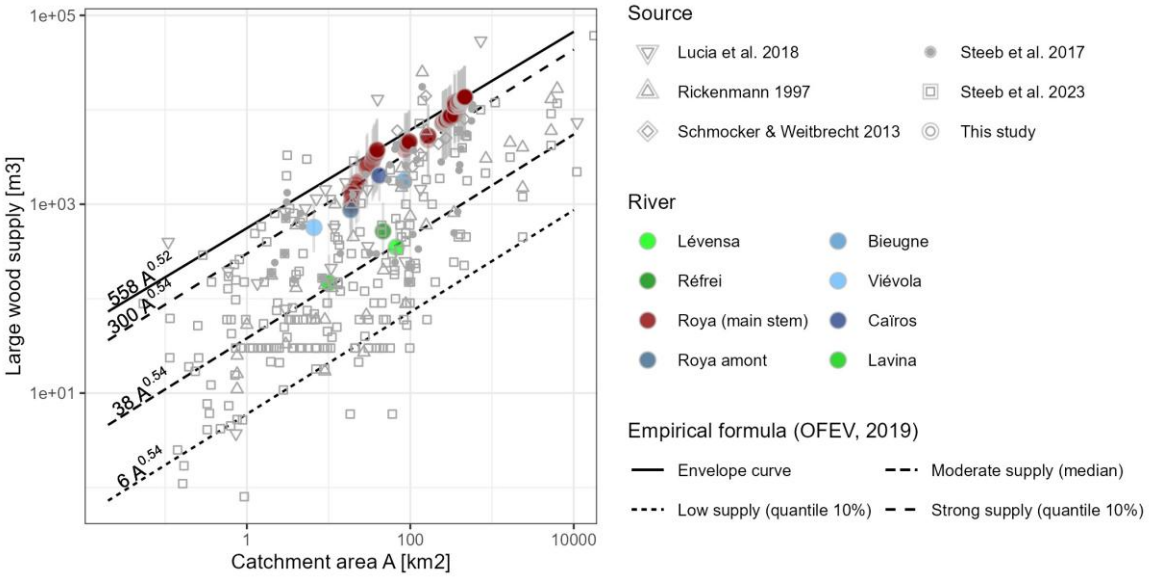

Figure 10: Large wood supply versus catchment area for the studied reaches and data from the literature (Rickenmann 1997, Schmocker, Weitbrecht 2013, Steeb et al. 2017, 2023, Lucía et al. 2018)

In line with this work, the OFEV guide (2019, p. 28) provides simple empirical formulas, with one or two parameters, making it possible to predict the supply of large wood in relation to catchment morphometric parameters (area, length of the main drain) or parameters describing the magnitude of the flood (peak flow, hydrograph volume, rainfall volume, volume of associated bedload transport). Since the large wood production process is highly random, the guide systematically proposes four formulas: a mean adjustment representative of moderate supply, adjustments greater than 10% and 90% of peaks, representative of relatively low and strong supply volumes, as well as an envelope curve, representative of extreme supply. This approach, well adapted to the high variability of the phenomenon, provide ranges of the potential large wood supply, also allowing the user to gauge the precision of the estimations. The adjustments to the catchment size-dependent equations of the OFEV guide (2019, p.28) are illustrated in Figure 10. The supply of the least active of the Roya's tributaries was equivalent to a "moderate supply" (Lévensa, Réfrei, Lavina valleys), whereas the supply of the most active tributaries approaches a "strong supply" (Bieugne, Viévola, Roya amont, and Caïros Valley). Finally, it can be observed that the peaks associated with the main stem of the Roya are globally between the "strong supply" adjustment and the envelope curve. This observation shows the relatively exceptional nature of this episode's large wood supply, given the extreme nature of the Storm Alex, the strong longitudinal slope of the hydrographic regime, and the presence of a riparian tree with a fairly dense canopy (57%). It should be noted, however, that these values remain predictable with these simple approaches considering a scenario with a substantial large wood supply.

4.4 Perspectives for future analyses

During the field visit in October 2021 (see details in Section S2), we observed that despite the violence of the Storm Alex, vegetation recolonization had begun one year after the storm in the valley bottoms. However, the earthwork to install protective structures and reestablish roads disturbed this resurgence. The intense disturbances of the natural recovery exposed the riparian trees to a reduction in floral species: invasive and cosmopolitan species have a more rapid installation and development capacity than local and specialist species. Even though the number of cases inventoried was low, they illustrate the different stages of vegetation succession one year after the Storm Alex along a bioclimatic gradient and suggest the utility of following up the dynamics observed.

Another to explore in future analyses would be the correlation between a substantial quantity of large wood deposited in the valley floors and the localization and state of bridges as well as overflows related to their obstruction. Large wood is indeed the main contributor to the formation of large wood jams obstructing bridges. Flows were thus deviated toward the banks and the upstream water levels increased, favoring outflanking of the structures and erosion of their abutments. The obstructions had an even greater effect in that the channel was initially narrow and was substantially widened with the flood, corresponding to the maximum rainfall intensity in the Tende sector. The reconstruction of the bridges in progress is responding to this problem and the bridge spans were generally increased so as to allow passage of a flood equivalent to the Storm Alex, including the transported large wood (CD06, 2021).

5 Conclusion

This article presents a detailed analysis of the large wood fluxes from the French Roya catchment following the Storm Alex. The method developed is generalizable to other regions and sites, most particularly in France to the extent that data from the National Forest Inventory are used. Analog data exist in other regions of the world.

The analysis of the sources of large wood is based on digitization of the extents of active channels before and after flooding. This type of analysis is standard in river geomorphology studies and showcases these data by crossing them with forest inventories. The analysis of large wood deposits, conducted as exhaustively as possible for the present study, could be conducted more superficially using rapid surveys of the main accumulations observed in the field. Automatic detection methods could also be developed base on our dataset. The present case study of the Roya subjected to the Storm Alex concludes in a highly significant export of large wood volumes toward the sea. These conclusions are specific to this case study: other sites do not export volumes because of the presence of obstacles trapping the large wood load (structures, lake). These obstacles then allow completing the assessment, as we have attempted to do with satellite images.

This study presents the potential supply of an intermediate-sized alpine river (the catchment covering a few hundred square kilometers). In summary, we estimate that the Roya catchment exported a very significant volume of large wood at the scale of the flood associated with the Storm Alex. This volume exported by the French part of the river was: (i) at a minimum on the order of 7,000 m³ (very low estimation with a low assumption on the standing tree volumes and a high assumption on the diameter of the deposited pieces); (ii) the intermediate estimation on the order of 14,000 m³ (based on the intermediate standing tree volumes and the intermediate diameter of the deposited pieces); and (iii) the maximum estimations reaching 29,500 m³ (high standing tree volumes and low diameter of the deposited pieces).

The mean net supply of large wood was therefore on the order of 300 m³/km of geomorphologically active section (range of uncertainty, 100–500 m³/km) and 36 m³/km² of catchment (range of uncertainty, 18–75 m³/km²). This supply was compared to the literature data: it is undoubtedly high but remains equivalent to the most active of the other floods observed. Simple empirical methods characterizing high or very high large wood supply thus correctly predict the order of magnitude of this event. Improved comprehension of the biological and geomorphological processes associated with these events is indeed indispensable at the time of reconstruction and ecological restoration of the valleys, and in a context of warming of the Mediterranean Sea, in the future increasing the risk of violent rainfall episodes in this alpine valley.

Acknowledgements

This study was funded by the Direction Générale de la Prévention des Risques of the Ministère de la Transition Ecologique for the initial work. This article received funding from The European Union, the France–Italy INTERREG V-A program (ALCOTRA) 2014–2020 through the "RITA" n.8504 project for the complementary analysis work, as well as UCA CSI 2021 (MarAlpiSedi project) funding. The authors extend their thanks to colleagues at the Restauration des Terrains de Montagne department for their assistance and investment in the initial analysis, to Nicolas STEEB (WSL) for sharing the data on the reduction factor, to the Sentinel Hub EO Browser for making the Sentinel-2 L2A images available, as well as to the Italian Protezione Civile and the company Drone De Regard for having generously provided the drone images of Ventimiglia and the Caïros River. We warmly thank all of the colleagues who provided useful advice, notably Jean-Matthieu Monnet, Rose Rodier, Paul Passy, as well as students from the Master 1 ETTES program (Sorbonne Université) who participated in the field mission in October. Finally, this paper benefit from helpful comments by Jon Tunnicliffe and an anonymous reviewer, many thanks to both.

Data availability statement

All data used in this study are available upon reasonable request to the corresponding author. Many maps are yet provided in the appendix of ONF-RTM et al. (2022a) available at https://doi.org/10.57745/B69M2O.

Declaration of interests

The authors declare that they have no known competing financial interests or personal relationships that could have appeared to influence the work reported in this paper.

References

Arnaud-Fassetta, G., Cossart, E., Fort, M., 2005. Hydro-geomorphic hazards and impact of man-made structures during the catastrophic flood of June 2000 in the Upper Guil catchment (Queyras, Southern French Alps). Geomorphology 66, 41–67. https://doi.org/10.1016/j.geomorph.2004.03.014

Astrade, L., Jacob-Rousseau, N., Bravard, J.-P., Allignol, F., Simac, L., 2011. Detailed chronology of mid-altitude fluvial system response to changing climate and societies at the end of the Little Ice Age (Southwestern Alps and Cévennes, France). Geomorphology 133, 100–116.

Braudrick, C.A., Grant, G.E., Ishikawa, Y., Ikeda, H., 1997. Dynamics of wood transport in streams: A flume experiment. Earth Surface Processes and Landforms 22, 669–683. https://doi.org/10.1002/(SICI)1096-9837(199707)22:7<669::AID-ESP740>3.0.CO;2-L

Bravard, J.-P., Petit, F., 1997. Les cours d'eau, dynamique du système fluvial, Collection U. Armand Colin, Paris, France.

BRGM-SCP, 2006. Faisabilité de la mise en place d'un système d'annonce des crues sur la Roya. PIC INTERREG III A 2000-2006 ALCOTRA : EUROBASSIN.

Carrega, P., Michelot, N., 2021. Une catastrophe hors norme d'origine météorologique le 2 octobre 2020 dans les montagnes des Alpes-Maritimes. Physio-Géo 1–70. https://doi.org/10.4000/physio-geo.12370

CD06, 2021. Vallée de la Roya - Informations chantiers.

CEREMA, 2021. RETEX technique ALEX - Inondations des 2 et 3 octobre 2020 - Consensus hydrologique (No. 20- ME- 0354 (V1)). DDTM06.

Chmiel, M., Godano, M., Piantini, M., Brigode, P., Gimbert, F., Bakker, M., Courboulex, F., Ampuero, J.-P., Rivet, D., Sladen, A., Ambrois, D., Chapuis, M., 2022. Brief communication: Seismological analysis of flood dynamics and hydrologically triggered earthquake swarms associated with Storm Alex. Nat. Hazards Earth Syst. Sci. 22, 1541–1558. https://doi.org/10.5194/nhess-22-1541-2022

Church, M., Ferguson, R., 2015. Morphodynamics: Rivers beyond steady state. Water Resources Research 51, 1883–1897. https://doi.org/10.1002/2014WR016862

Church, M., Jakob, M., 2020. What Is a Debris Flood? Water Resources Research 56. https://doi.org/10.1029/2020WR027144

Comiti, F., 2012. How natural are Alpine mountain rivers? Evidence from the Italian Alps. Earth Surface Processes and Landforms 37, 693–707. https://doi.org/10.1002/esp.2267

Comiti, F., Lucía, A., Rickenmann, D., 2016. Large wood recruitment and transport during large floods: A review. Geomorphology 269, 23–39. https://doi.org/10.1016/j.geomorph.2016.06.016

Deleuze, C., Morneau, F., Renaud, J.P., Vivien, Y., Rivoire, M., Santenoise, P., Longuetaud, F., Mothe, F., Hervé, J.C., Vallet, P., 2014. Estimer le volume total d'un arbre, quelles que soient l'essence, la taille, la sylviculture, la station. Rendez-vous Techniques de l'ONF 22–32.

Dufour, S., Moulin, B., Piégay, H., 2003. Doit-on promouvoir systématiquement l'entretien des lits fluviaux et de leurs marges. Forêt méditerranéenne 24, 335–345.

Eysn, L., Hollaus, M., Lindberg, E., Berger, F., Monnet, J.-M., Dalponte, M., Kobal, M., Pellegrini, M., Lingua, E., Mongus, D., Pfeifer, N., 2015. A Benchmark of Lidar-Based Single Tree Detection Methods Using Heterogeneous Forest Data from the Alpine Space. Forests 6, 1721–1747. https://doi.org/10.3390/f6051721

Friedrich, H., Ravazzolo, D., Ruiz-Villanueva, V., Schalko, I., Spreitzer, G., Tunnicliffe, J., Weitbrecht, V., 2021. Physical modelling of large wood (LW) processes relevant for river management: Perspectives from New Zealand and Switzerland. Earth Surface Processes and Landforms esp.5181. https://doi.org/10.1002/esp.5181

Gasser, E., Schwarz, M., Simon, A., Perona, P., Phillips, C., Hübl, J., Dorren, L., 2019. A review of modeling the effects of vegetation on large wood recruitment processes in mountain catchments. Earth-Science Reviews 194, 350–373. https://doi.org/10.1016/j.earscirev.2019.04.013

Gschnitzer, T., Gems, B., Mazzorana, B., Aufleger, M., 2017. Towards a robust assessment of bridge clogging processes in flood risk management. Geomorphology 279, 128–140. https://doi.org/10.1016/j.geomorph.2016.11.002

Gurnell, A.M., Piégay, H., Swanson, F.J., Gregory, S.V., 2002. Large wood and fluvial processes: Large wood and fluvial processes. Freshwater Biology 47, 601–619. https://doi.org/10.1046/j.1365-2427.2002.00916.x

JCGM, 2008. Evaluation of measurement data — Guide to the expression of uncertainty in measurement (No. JCGM 100:2008). Joint Committee for Guides in Metrology.

Kriegler, F.J., Malila, W.A., Nalepka, R.F., Richardson, W., 1969. Preprocessing Transformations and Their Effects on Multispectral Recognition, in: Proceedings of the Sixth International Symposium on Remote Sensing of Environment. pp. 97–132.

Lallias-Tacon, S., Liébault, F., Piégay, H., 2017. Use of airborne LiDAR and historical aerial photos for characterising the history of braided river floodplain morphology and vegetation responses. CATENA 149, 742–759. https://doi.org/10.1016/j.catena.2016.07.038

Lassettre, N.S., Kondolf, G.M., 2011. Large woody debris in urban stream channels: redefining the problem. River Research and Applications 28, 1477–1487. https://doi.org/10.1002/rra.1538

Liébault, F., Gomez, B., Page, M., Marden, M., Peacock, D., Richard, D., Trotter, C.M., 2005. Land-use change, sediment production and channel response in upland regions. River Research and Applications 21, 739–756. https://doi.org/10.1002/rra.880

Liébault, F., Piégay, H., 2002. Causes of 20th century channel narrowing in mountain and piedmont rivers of Southeastern France. Earth Surface Processes and Landforms 27, 425–444. https://doi.org/10.1002/esp.328

Livers, B., Lininger, K.B., Kramer, N., Sendrowski, A., 2020. Porosity problems: comparing and reviewing methods for estimating porosity and volume of wood jams in the field. Earth Surf. Process. Landforms esp.4969. https://doi.org/10.1002/esp.4969

Lucía, A., Comiti, F., Borga, M., Cavalli, M., Marchi, L., 2015. Dynamics of large wood during a flash flood in two mountain catchments. Natural Hazards and Earth System Sciences 15, 1741–1755. https://doi.org/10.5194/nhess-15-1741-2015

Lucía, A., Schwientek, M., Eberle, J., Zarfl, C., 2018. Planform changes and large wood dynamics in two torrents during a severe flash flood in Braunsbach, Germany 2016. Science of The Total Environment 640–641, 315–326. https://doi.org/10.1016/j.scitotenv.2018.05.186

Macchione, F., Lombardo, M., 2021. Roughness-Based Method for Simulating Hydraulic Consequences of Both Woody Debris Clogging and Breakage at Bridges in Basin-Scale Flood Modeling. Water Resources Research 57. https://doi.org/10.1029/2021WR030485

Mazzorana, B., Hübl, J., Zischg, A., Largiader, A., 2011. Modelling woody material transport and deposition in alpine rivers. Natural Hazards 56, 425–449. https://doi.org/10.1007/s11069-009-9492-y

Mazzorana, B., Ruiz-Villanueva, V., Marchi, L., Cavalli, M., Gems, B., Gschnitzer, T., Mao, L., Iroumé, A., Valdebenito, G., 2018. Assessing and mitigating large wood-related hazards in mountain streams: recent approaches. Journal of Flood Risk Management 11, 207–222. https://doi.org/10.1111/jfr3.12316

Melun, G., Liébault, F., Piton, G., Chapuis, M., Passy, P., Martins, C., Kuss, D., 2022. Crues exceptionnelles de la Vésubie et de la Roya (octobre 2020): caractérisation hydrogéomorphologique et perspectives de gestion - Major floods of the Vésubie and Roya Rivers (Alps, France) in October 2020: hydrogeomorphological caracterisation and management perspectives, in: Proc. of the 4th International Conference I.S.Rivers. Presented at the IS Rivers, GRAIE, Lyon, France, p. 22.

Monnet, J.M., 2020. lidaRtRee: Forest Analysis with Airborne Laser Scanning (Lidar) Data.

OFEV, 2019. Bois flottant dans les cours d'eau (No. Connaissance de l'environnement num 1910). Office fédéral de l'environnement, Berne.

Okamoto, T., Takebayashi, H., Sanjou, M., Suzuki, R., Toda, K., 2019. Log jam formation at bridges and the effect on floodplain flow: A flume experiment. Journal of Flood Risk Management 13, e12562. https://doi.org/10.1111/jfr3.12562

ONF-RTM, ONF-DRN, INRAE-ETNA, 2022a. Retour d'expérience technique de la crue du 2 octobre 2020 dans la vallée de la Roya - Volet torrentiel (No. V1). Direction Départementale des Territoires et de la Mer des Alpes-Maritimes (DDTM06), Nice (France). 275 pp. +922 appendixes [online] https://doi.org/10.57745/B69M2O (last visited 10/31/2023)

ONF-RTM, ONF-DRN, INRAE-ETNA, 2022b. Retour d'expérience technique de la crue du 2 octobre 2020 dans la vallée de la Vésubie - Volet torrentiel (No. V1). Direction Départementale des Territoires et de la Mer des Alpes-Maritimes (DDTM06), Nice (France). 299pp + 1540 appendixes. [online] https://doi.org/10.57745/UGJZWT (last visited 10/31/2023)

Payrastre, O., Nicolle, P., Bonnifait, L., Brigode, P., Astagneau, P., Baise, A., Belleville, A., Bouamara, N., Bourgin, F., Breil, P., Brunet, P., Cerbelaud, A., Courapied, F., Devreux, L., Dreyfus, R., Gaume, E., Nomis, S., Poggio, J., Pons, F., Rabab, Y., Sevrez, D., 2022. Tempête Alex du 2 octobre 2020 dans les Alpes-Maritimes : une contribution de la communauté scientifique à l'estimation des débits de pointe des crues. LHB 2082891. https://doi.org/10.1080/27678490.2022.2082891

Piégay, H., Dupont, P., Bravard, J.-P., 1994. 1. -Les ripisylves et les crues dans la France du sud-est : de l'histoire à la gestion contemporaine. Journées de l'hydraulique 23, 277–288.

Piégay, H., Moulin, B., Hupp, C.R., 2017. Assessment of transfer patterns and origins of in-channel wood in large rivers using repeated field surveys and wood characterisation (the Isère River upstream of Pontcharra, France). Geomorphology 279, 27–43. https://doi.org/10.1016/j.geomorph.2016.07.020

Quiniou, M., Piton, G., Ruiz-Villanueva, V., Péririn, C., Savatier, J., Bladé, E., 2022. Wood Debris Risk Analysis and Protection Scenarios of Lourdes City Using Iberwood Model, in: Gourbesville, P., Caignaert, G. (Eds.), Advances in Hydroinformatics. Springer Water, p. 19.

Ravazzolo, D., Mao, L., Picco, L., Lenzi, M.A., 2015. Tracking log displacement during floods in the Tagliamento River using RFID and GPS tracker devices. Geomorphology 228, 226–233. https://doi.org/10.1016/j.geomorph.2014.09.012

Rey, T., Chevret, C., Candela, T., Robustelli, M., 2022. Leçons tirées de la crue torrentielle catastrophique du 2 octobre 2020 dans la vallée de la Vésubie (Alpes-Maritimes, France). Physio-Géo 193–223. https://doi.org/10.4000/physio-geo.14922

Rickenmann, D., 1997. Schwemmholz und hochwasser [Driftwood and floods]. Wasser, Energie, Luft - Eau, Energie, Air 89, 115–119.

Rickli, C., Badoux, A., Rickenmann, D., Steeb, N., Waldner, P., 2018. Large wood potential, piece characteristics, and flood effects in Swiss mountain streams. Physical Geography 1–23. https://doi.org/10.1080/02723646.2018.1456310

Roux, C., Alber, A., Bertrand, M., Vaudor, L., Piégay, H., 2015. "FluvialCorridor": A new ArcGIS toolbox package for multiscale riverscape exploration. Geomorphology 242, 29–37. https://doi.org/10.1016/j.geomorph.2014.04.018

Ruiz-Villanueva, V., Bodoque, J.M., Díez-Herrero, A., Bladé, E., 2014. Large wood transport as significant influence on flood risk in a mountain village. Natural Hazards 74, 967–987. https://doi.org/10.1007/s11069-014-1222-4

Ruiz-Villanueva, V., Piégay, H., Gurnell, A.M., Marston, R.A., Stoffel, M., 2016. Recent advances quantifying the large wood dynamics in river basins: New methods and remaining challenges. Reviews of Geophysics 54, 611–652. https://doi.org/10.1002/2015rg000514

Ruiz-Villanueva, V., Wyżga, B., Mikuś, P., Hajdukiewicz, M., Stoffel, M., 2017. Large wood clogging during floods in a gravel-bed river: the Dlugopole bridge in the Czarny Dunajec River, Poland. Earth Surface Processes and Landforms 42, 516–530. https://doi.org/10.1002/esp.4091

SABO Division, 2000. Guideline for driftwood countermeasures (proposal and design). Ministry of Construction. Japan.

Schmocker, L., Weitbrecht, V., 2013. Driftwood: Risk analysis and engineering measures. Journal of Hydraulic Engineering 139, 683–695. https://doi.org/10.1061/(ASCE)HY.1943-7900.0000728

SMIAGE, 2021. Rapport d'activité SMIAGE MARALPIN 2020. Syndicat Mixte Inondations, Aménagement et Gestion de l'Eau Maralpin.

Steeb, N., Rickenmann, D., Badoux, A., Rickli, C., Waldner, P., 2017. Large wood recruitment processes and transported volumes in Swiss mountain streams during the extreme flood of August 2005. Geomorphology 279, 112–127. https://doi.org/10.1016/j.geomorph.2016.10.011

Steeb, N., Ruiz-Villanueva, V., Badoux, A., Rickli, C., Mini, A., Stoffel, M., Rickenmann, D., 2023. Geospatial modelling of large-wood supply to rivers: a state-of-the-art model comparison in Swiss mountain river catchments. Earth Surface Dynamics 11, 487–509. https://doi.org/10.5194/esurf-11-487-2023

Williams, P.F., Rust, B.R., 1969. The Sedimentology of a Braided River. Journal of Sedimentary Research 39, 649–679.

Wohl, E., Kramer, N., Ruiz-Villanueva, V., Scott, D.N., Comiti, F., Gurnell, A.M., Piegay, H., Lininger, K.B., Jaeger, K.L., Walters, D.M., Fausch, K.D., 2019. The Natural Wood Regime in Rivers. BioScience 69, 259–273. https://doi.org/10.1093/biosci/biz013